Transport Selectivity of Tribenuron-Methyl Imprinted Polymer Nanowire Membrane Prepared Using *N,O*-bismethacryloyl Ethanolamine as a Functional Crosslinking Monomer

Xufei Liu, Jie Zhou, Changbao Chen

Department of Material Chemistry, College of Chemistry and Material Science, Shandong Agricultural University, Taian 271018, China

Received 3 December 2009; accepted 14 March 2010
DOI 10.1002/app.32456
Published online 24 May 2010 in Wiley InterScience (www.interscience.wiley.com).

ABSTRACT: Using tribenuron-methyl as a template and *N,O*-bismethacryloyl ethanolamine as a functional crosslinking monomer, a molecularly imprinted nanowire membrane was prepared over an anodic alumina oxide membrane. The nanowire fabric of the imprinted membrane was established with a scanning electron microscope and a transmission electron microscope. However, the nonimprinted particulate membrane is formed in the absence of a template. Scatchard analysis showed that an equal class of binding sites were formed in the imprinted nanowire membrane and the dissociation constant and the maximum number of these binding sites were estimated to be 1.44×10^{-5} M and 22.7 μmol/g, respectively. The permeation experiments throughout the imprinted membrane and the nonimprinted one were carried out in a solution containing the template and its competitive analogs. These results demonstrated that the molecularly imprinted nanowire membrane exhibited higher transport selectivity for the template tribenuron-methyl than its analogs, chlorimuron-ethyl, thifensulfuron-methyl and *N*-(4-bromophenylcarbamoyl)-5-chloro-1H-benzo[d]imidazole-2-carboxamide. But the nonimprinted granular membrane had no permselectivity for the four substrates. © 2010 Wiley Periodicals, Inc. J Appl Polym Sci 118: 678–684, 2010

Key words: tribenuron-methyl; *N,O*-bismethacryloyl ethanolamine; molecularly imprinted nanowire membrane; transport selectivity

INTRODUCTION

Tribenuron-methyl a sulfonylurea herbicide can efficiently control broad-leafed weeds and some grasses in cereals like wheat, barley, and oat, and is widely used for a variety of crops because of its high herbicidal activity and low toxicity for mammals. It has low use ranges (10–100 g of active ingredient/ha) and is rapidly degraded in soil.[1,2] Therefore, the concentration of this herbicide usually found in environmental soil and water is very low (ppt or ppb range). On the other hand, the structures of all sulfonylureas are very similar, and they may be present as a mixture of several compounds. For these reasons and because of their chemical and thermal instability, individual recognition of a series of sulfonylurea herbicides in environmental samples is a particularly challenging problem.

Molecularly imprinting is a technique for preparing "memory effect" polymers containing specific recognition sites toward template molecules.[3] It originally comes from "lock-and-key hypothesis" and has already been used for mimicking natural receptors[4] and for the synthesis of polymers carrying binding sites with high affinity toward drugs, small analytes, peptides, and proteins.[5–8] Molecularly imprinted polymer membranes (MIPMs) have more accessible binding sites, a faster rate of mass transfer and faster binding kinetics compared to traditional bulky molecularly imprinted polymers. Their stability, mechanical strength, and selectivity are significantly better than those of biological membranes. However, these materials are not widely used because their preparation is less straightforward and requires specially adapted protocols.[9] So the preparation of MIPMs has aroused increasing attention.[10–12] Mosbach and coworkers[13] have introduced a noteworthy method for creating MIPMs based on oriented immobilization of the template molecules on porous silica beads before polymerization. This method has been further developed by Sellergren for the imprinting of amino acids and peptides.[14,15] Recently, Wang's group has also reported a similar approach for creating molecularly imprinted nanowire membranes by immobilization of the template molecules within the pores of a nanoporous alumina membrane. This nanowire membrane is relatively monodispersed and has a moderately high imprinting

Correspondence to: J. Zhou (zhoujie@sdau.edu.cn).
Contract grant sponsor: The National High-tech R & D Program (863 program); contract grant number: 2007AA10Z432.
Contract grant sponsor: National Natural Science Foundation of China; contract grant number: 30871756.

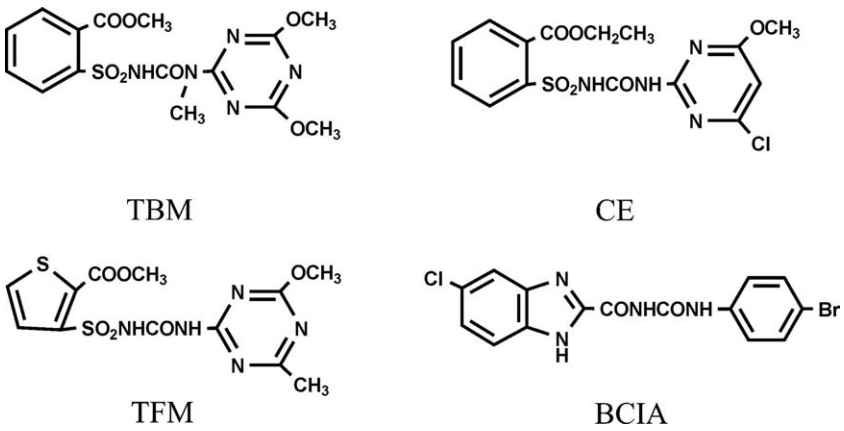

Figure 1 Molecular structures of tested substrates.

surface area.[16,17] However, the methodology of MIPM formation mentioned above requires optimization of the complicated MIPM components, including which functional monomers to use, what type of crosslinker to use, the optimum ratio of functional monomer/crosslinker, and the optimum ratio of functional monomer/template. The best results for the formation of MIPMs can only be determined by empirical optimization via synthesis and evaluation of several polymer membranes. This process is very time-consuming and not yet generalized for any target, which has limited the broader application of MIPMs. Recently, the Spivak group has discovered a simple approach to molecular imprinting which uses a single crosslinker, *N,O*-bismethacryloyl ethanolamine (NOBE) along with template, initiator, and solvent. This formulation eliminates the need for additional functional monomers and empirical optimization of relative ratios of functional monomers, crosslinkers, and templates. Furthermore, utilization of NOBE alone often provides molecularly imprinted polymers with higher affinity toward templates than those of incorporating a functional monomer (for example, methacrylic acid).[18] In this report, we presented a technique for the synthesis of a MIP nanowire membrane using the single crosslinking monomer NOBE and a template (tribenuron-methyl) by surface-initiated atom transfer radical polymerization (ATRP).[19] In comparision of the imprinted membrane versus the nonimprinted membrane, the MIP nanowire membrane exhibited higher affinity and permselectivity for the template tribenuron-methyl than its analogs, chlorimuron-ethyl, thifensulfuron-methyl, and *N*-(4-bromophenylcarbamoyl)-5-chloro-1H-benzo[d]imidazole-2-carboxamide.

EXPERIMENTAL

Materials and instruments

Materials

A commercially anodic alumina oxide (AAO) membrane with a thickness of 60 μm and a pore diameter of 100 nm was purchased from Whatman. Tribenuron-methyl (99.7%, TBM), chlorimuron-ethyl (99.8% CE), thifensulfuron-methyl (99.4%, TFM) and *N*-(4-bromophenylcarbamoyl)-5-chloro-1H-benzo[d]imidazole-2-carboxamide (99.0%, BCIA) were generously provided by College of Plant Protection Science, Shandong Agricultural University (Taian, China). Their chemical structures were shown in Figure 1. 3-Aminopropyltrimethoxysilane, α-bromoisobutyryl bromide, methacryloyl chloride, and trifluoroacetic acid were purchased from Aladdin. 1,4,8,11-Tetraazacyclotetradecane was purchased from Fluka. HPLC-grade acetonitrile and methanol were purchased from Tianjin Yongda Chemical Reagent Development Center. Tetrahydrofuran (THF), triethylamine, ethanolamine, and toluene were purchased from Basifu Chemical Co. Methylene dichloride, anhydrous ethanol, acetic acid, ethyl acetate, *n*-hexane, sodium citrate, sodium bicarbonate, and anhydrous sodium sulfate were purchased from Tianjin Kaitong Chemical Reagent Co. Methacryloyl chloride was distilled to remove the inhibitor before use. Methylene dichloride, triethylamine were dried by refluxing over CaH_2, followed by distillation.

Instruments

The elemental analysis was carried out using a Vario III Elementary Analyzer. ^{1}H-NMR and IR were recorded using a Bruker DPX300 FT-NMR machine and a Nicolet 380 FTIR spectrometer. Polymer batch binding and permselective studies were performed using a Shimadzu UV–2450 double-beam spectrophotometer or a Waters HPLC system (a pump, Model 600; a manual injector, Model Rheodyne 7725i; CAPCELL PAK C_{18} column, 250 mm × 4.6 mm i.d.; Model 2487 UV absorbance detector). Morphologies of polymeric membranes were characterized using an H-8010 scanning electron microscope and an H-800 transmission electron microscope.

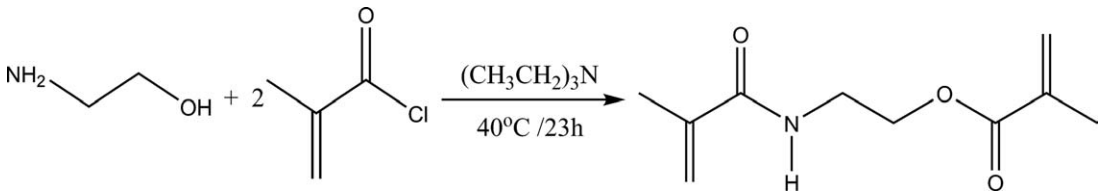

Figure 2 Synthetic scheme of NOBE.

Synthesis of NOBE

Synthesis of this monomer was performed according to a literature procedure[20] as shown in Figure 2, with slight modification. Et_3N (3.74 g, 5.15 mL, 37 mmol) was added dropwise over 5 min at 0°C to a solution of ethanolamine (0.976 g, 16 mmol) in dry methylene dichloride (15 mL) with stirring under N_2, and then methacryloyl chloride (3.876 g, 3.6 mL, 37 mmol) was added dropwise with vigorous stirring. After completing addition of methacryloyl chloride, the reaction mixture was increased to 40°C and was stirred for 23 h at this temperature. The mixture was filtered out and the precipitate (Et_3NHCl) discarded. The filtrate was washed three times with 0.5*M* sodium bicarbonate (3 × 15 mL) and 0.5*M* sodium citrate (3 × 15 mL) in turn, then dried over anhydrous sodium sulfate. After evaporation of the solvent and drying of the compound in a vacuum oven overnight, a pale yellow oil was obtained in 72.6% yield (g). ^{1}H-NMR (300 MHz, $CDCl_3$): δ = 6.48 ppm (s, 1 H); 6.12 ppm (s, 1 H); 5.70 ppm (s, 1 H); 5.60 ppm (s, 1 H); 5.33 ppm (s, 1 H); 4.30 ppm (t, 2 H); 3.64 ppm (quad, 2 H); 1.96 ppm (s, 3 H); 1.94 ppm (s, 3 H). IR (KBr), ν/cm^{-1}: 3346[ν(N—H)]; 1784, 1709 [ν(C=O)]; 1662, 1623 [ν(C=C)]; 1296 [ν(C—N)]; 1168 [ν(C—O)]. Anal. Calcd. for $C_{10}H_{15}O_3N$: C, 60.52; H, 7.12; N, 7.27. Found: C, 60.89; H,7.67; N, 7.10.

Preparation of the AAO membrane with the immobilized ATRP initiator

The AAO membrane with a thickness of 60 μm and a pore diameter of 100 nm was first modified with an aminopropylsilane. The AAO membrane was soaked in a solution including 0.5 mL of 3-aminopropyltrimethoxysilane, 2.8 mL of ethanol, and 0.2 mL of sodium acetate buffer solution (50 m*M*, pH 5.0). The solution was placed under vacuum for 5 min to remove air from the pores in the membrane. The silanization reaction was terminated after another 15 min by rinsing with ethanol. The membrane was then cured by heating in vacuum at 150°C for 1 h. The freshly made aminopropyl group-modified AAO membrane was immersed in 4 mL of dry methylene dichloride containing dry triethylamine (4%, v/v). Afterward, 4 mL of dry methylene dichloride containing 0.016 mL of α-bromoisobutyryl bromide was slowly dropped into the solvent. The mixture was kept for 2 h at 0°C and then for 12 h at room temperature. The AAO membrane was repeatedly rinsed with acetone and toluene before being dried under vacuum.

Preparation of TBM-imprinted nanowire membrane (P_{TWM})

TBM (0.05 mmol) and NOBE (4.5 mmol) were dissolved in 8 mL of THF. The solution was stirred for 2 h at room temperature for the formation of a complex of the template molecule TBM and the functional crosslinked monomer NOBE. Without extra functional monomers added, the mixture was then purged with N_2 for 15 min and injected into a sealed glass bottle containing ATRP initiator immobilized AAO membrane and the organometallic catalyst obtained by mixing CuBr (2 μmol) with 1,4,8,11-tetra-azacyclotetradecane (4 μmol). This reaction system was incubated at 70°C under N_2 for 24 h. The AAO membrane was washed with methanol–acetic acid (9 : 1, v/v) and methanol in sequence before drying under vacuum. After dissolving the AAO membrane from the resultant polymer membrane with 1*M* sodium hydroxide solution, the microscopic analyses of the membrane were carried out by using a scanning electron microscope (SEM) and a transmission electron microscope (TEM).

The reference (nonimprinted) polymer membrane (P_{RM}) was prepared in the same way but in the absence of the template molecule and worked up by the same procedure.

P_{TWM} binding experiments

P_{TWM} or P_{RM} (17.0 mg) was placed into a flask and mixed with 3.0 mL of a series of known concentration of TBM in methanol. The flask was oscillated in a constant temperature bath oscillator for 24 h at 25°C. The concentration of free substrates in the solution was determined using HPLC with an eluent of acetonitrile/water/trifluoroacetic acid (50/50/0.1, v/v/v) at a flow rate of 1.0 mL/min and the detection wavelength 254 nm. The amount of TBM bound to P_{TWM}, Q was calculated by subtracting the concentration of free substrate from the initial substrate concentration. The average data of triplicate independent results were used for the following discussion.

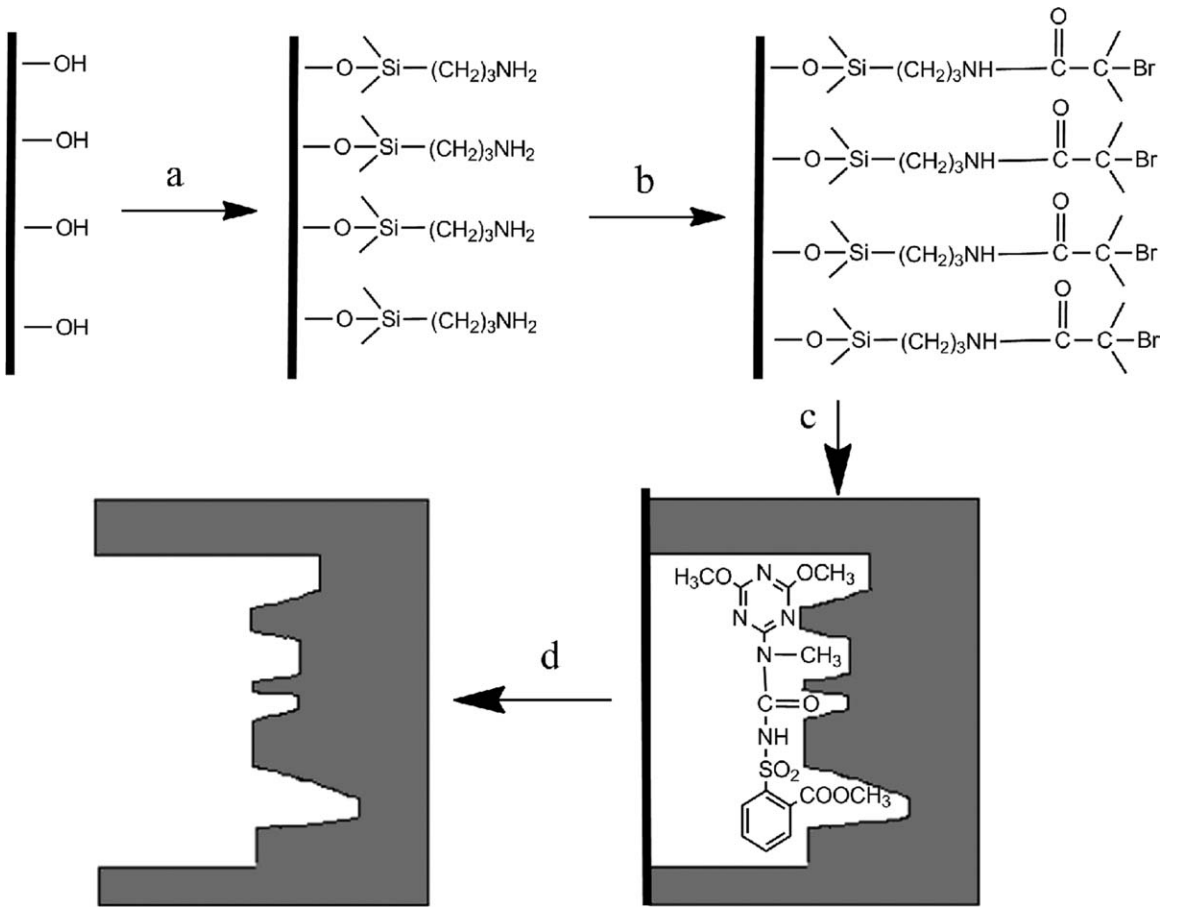

Figure 3 Scheme representation of the molecularly imprinted approach. (a) Silanization with 3-aminopropltrimethoxysilane, (b) Reaction with α-bromoisobutyryl bromide, (c) Plolymerization of TBM-NOBE complexes and NOBE, (d) Removal of TBM.

Membrane transport experiments

The membranes were mounted between the two stirred chambers in an H-shaped two-compartment cell with constant stirring. 35 mL of a methanol solution, which was $5.0 \times 10^{-5} M$ in a substrate was placed in the feeding chamber, and pure methanol in the receiving chamber. The amount of the transported substrate was determined by UV spectrophotometric method. That is, an absorbance of the solution in the receiving chamber was measured at the maximum absorption wavelengths of substrates tested (CE: 238 nm, TFM: 247 nm, BCIA: 295 nm, TBM: 229 nm) every an hour using a 1-cm cell and methanol as a reference. The amounts of the transported substrates were calculated based on Beer's law. The mean values of three measurements were used in the following data analysis.

Evaluation of membrane separation performance

The polymeric membranes were placed between the same devices as the above transport experiments. A methanol solution consisting of $5.0 \times 10^{-5} M$ concentrations of TBM, TFM, CE, and BCIA was in the feeding chamber, and pure methanol in the receiving chamber. The amount of each transported substrate was quantified by HPLC with an eluent of acetonitrile/water/trifluoroacetic acid (50/50/0.1, v/v/v) at a flow rate of 1.0 mL/min and the detection wavelength 254 nm, then the selectivity factors could be calculated according to $\alpha_{ij} = c_i/c_j$, where c refers to the concentration of the transported substrate in the receiving chamber, i and j refer to the different substrates.

RESULTS AND DISCUSSION

Preparation of P_{TWM}

Recently, successful surface MIP nanowires have been reported.[11,16,17] In this study, the synthesis of the MIP nanowire membrane using a porous anodic alumina oxide (AAO) membrane by surface-initiated atom transfer radical polymerization (ATRP) was described. ATRP is based on the transfer of a halogen atom from the initiator to the monomer and the successive transfer to the growing polymer chain is

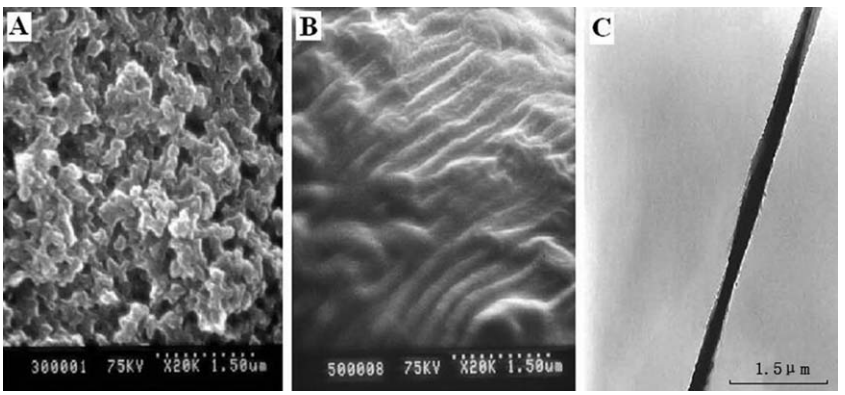

Figure 4 Scanning electron micrographs of P_{RM} (A) and P_{TWM} (B) and Transmission electron micrograph of P_{TWM} (C) after the removal of the alumina membranes by 1*M* NaOH solution.

catalyzed by the transition-metal complex that mediates the propagation. The AAO membrane with the immobilized ATRP initiators was prepared by a two-step method. The AAO membrane was first modified with 3-aminopropyltrimethoxysilane. The ATRP initiator, 2-bromo-2-methylpropionyl bromide, was then grafted onto the silanized AAO membrane. This AAO membrane was used as a macroinitiator in the subsequent molecular imprinting process as shown in Figure 3. The template molecule and the functional crosslinking monomer used in this study are TBM and NOBE, respectively. In the prepolymer solution, NOBE not only acts as a crosslinker, but also provides binding functionality that interacts with the template as well, presumably through hydrogen bonding via the amide group. The greater molecular recognition effect of P_{TWM} is afforded by the amide group of NOBE.

Morphology characterization of P_{TWM}

After polymerization and removal of the template molecules, the imprinted polymeric membrane attached to the AAO membrane was smooth and translucent by macroscopic observation. There was no difference between P_{TWM} and P_{RM} in visual topography at the macroscopic level. However, SEM and TEM results (Fig. 4) verified the formation of NOBE nanowires in P_{TWM} in the AAO membrane. The diameter of the nanowires was about 100 nm. In comparison with P_{TWM}, P_{RM} had obvious differences in morphology, which was granular. This demonstrates that the template TBM plays an important role in the formation of NOBE nanowires on the surface, which has a decisive impact on P_{TWM} transport selectivity.

Binding characteristics of P_{TWM}

To investigate the binding performance of P_{TWM}, the batch rebinding study of P_{TWM} was carried out in 1.0–9.0 $\times$ $10^{-5}M$ range of TBM initial concentrations. Binding isotherms are plotted as the concentration of TBM bound to P_{TWM} or P_{RM} vs. TBM free in solution (Fig. 5). Figure 5 showed that the concentration of bound TBM increased with increasing free concentration and the amounts of TBM bound to P_{TWM} were much higher than those bound to P_{RM}. In this range, the binding data obtained for P_{TWM} were dealt with by linear regression according to the Scatchard equation: $Q/[\mathrm{TBM}] = (Q_{max} - Q)/K_d$, where K_d is an equilibrium dissociation constant and Q_{max} an apparent maximum number of binding sites.

As shown in Figure 6, the obtained Scatchard plot was a reasonably straight line, the slope and intercept of which are equal to $-1/K_d$ and Q_{max}/K_d, respectively. This observation indicates that the binding sites in P_{TWM} are homogeneous in respect to the affinity for TBM and the nonspecific adsorption of P_{TWM} can be assumed to be small enough to ignore in this concentration range. The K_d and Q_{max} can be calculated to be 1.44 $\times$ $10^{-5}M$ and 22.7 μmol/

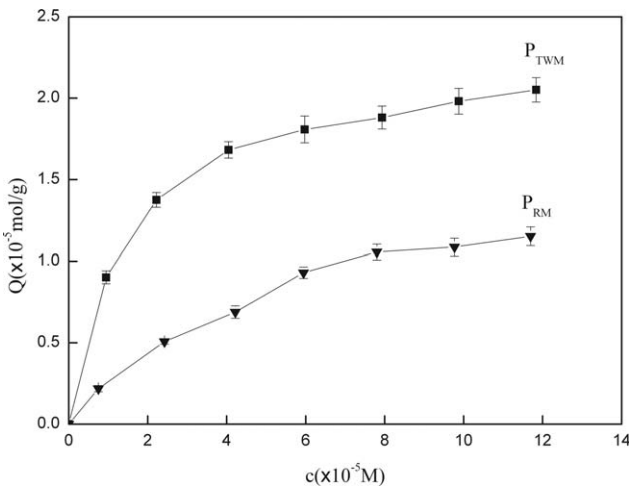

Figure 5 Binding isotherms of P_{TWM} and P_{RM} measured for their binding to TBM in methanol ($n = 3$).

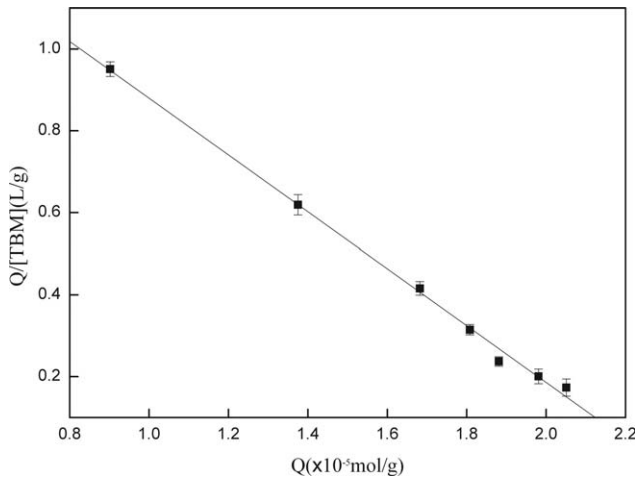

Figure 6 Scatchard plot for the homogeneous P_{TWM} ($n = 3$).

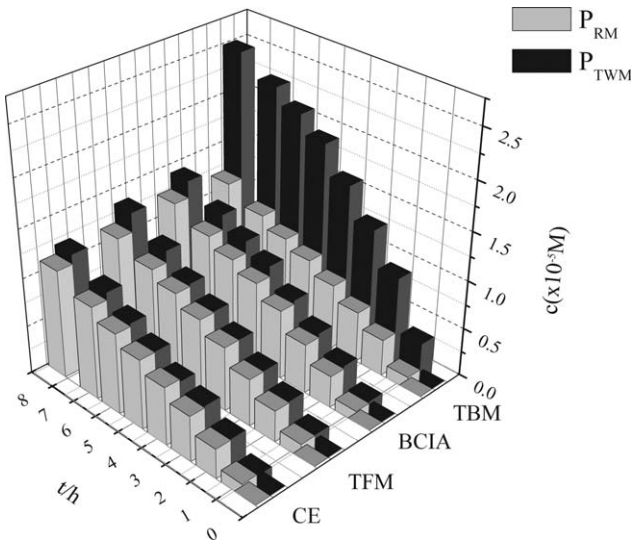

Figure 7 Time-transport selectivity of tested substrates through P_{TWM} (a) or P_{RM} (b). Substrate initial concentration in the feeding chamber is $5.0 \times 10^{-5}M$ and height of columns represents substrate concentration in the receiving chamber at various permeation time. The mean values of three measurements were used.

g from the slope and the intercept of the Scatchard plot, respectively.

Transport selectivity of P_{TWM}

To confirm the complementary relationship of the functional groups between the template molecules and the binding sites of P_{TWM}, the permselectivity of the imprinted nanowire membrane P_{TWM} was assessed by diffusion studies of the substrates TBM, TFM, CE, and BCIA, which are sulfonylurea herbicides. Figure 7 showed the diffusion fluxes of the substrates (in separate experiments) across P_{TWM} and P_{RM} at less than 5% of relative standard deviations ($n = 3$). Diffusion rates of the substrates across the molecularly nonimprinted membrane P_{RM} were significantly slow. Further, the four substrates diffused through P_{RM} at approximately the same rate. However, TBM diffused through the molecularly imprinted nanowire membrane P_{TWM} at a much higher rate than TFM, CE, or BCIA. These results indicate that the TBM-imprinted nanowire membrane P_{TWM} is permselective for the template TBM. This permselectivity of P_{TWM} derives from TBM binding sites situated at the surface of the nanowires produced on the basis of molecular imprinting.

Evaluation of membrane separation capacity

To better understand selectivity of the molecularly imprinted nanowire membrane P_{TWM}, we undertook competitive transport experiments with P_{TWM} and P_{RM}, where the four substrates TBM, TFM, CE, and BCIA were applied simultaneously. The concentration of each substrate in the receiving chamber was determined by HPLC and the selectivity factors were calculated. Values of the selectivity factors obtained were shown in Table I. Table I indicated that TBM was transported at a greater rate than BCIA, TFM, and CE, and the selectivity factors reached a constant value from 1.5 to 3 h in the permeation process, respectively, which of P_{TWM} for TBM/BCIA, TBM/TFM, and TBM/CE were 1.30, 1.50, and 1.64 at 3 h, respectively. However, the selectivity factors of P_{RM} were in the range of 1.04–0.95 for all substrates compared. This further demonstrates that P_{TWM} exhibits higher permselectivity for TBM.

The selective transport arises from a process that involves reversible complexation and exchange between TBM and the imprinted sites situated at the surface of the nanowires by hydrogen bonding interactions. Facilitated transport of TBM across the TBM-imprinted nanowire membrane is attributable to the complement of the functional groups between

TABLE I
Selective Factors for Tested Substrates in P_{TWM} and P_{RM} in Competitive Diffusion Experiments

	P_{TWM}			P_{RM}		
Time (h)	TBM/BCIA	TBM/TFM	TBM/CE	TBM/BCIA	TBM/TFM	TBM/CE
0.5	1.24	1.47	2.16	0.96	1.03	1.04
1.5	1.28	1.50	1.68	0.97	1.00	0.99
3.0	1.30	1.50	1.64	0.95	0.95	1.01

TBM and the imprinted sites.[21] Concentration differences serve as the driving force for molecular transport through the membranes. Substrate molecules bound to the membrane can either dissociate toward the receiving chamber or flow back into the feeding chamber. Because of the concentration gradient, most of the substrate molecules diffuse to the receiving chamber.[22] The functional groups of BCIA, TFM, and CE are not complementary to the imprinted sites of P_{TWM}, so there is weak complexation and slow exchange between BCIA, TFM, or CE and the imprinted sites in the nanowire membrane. This results in low transport rates when BCIA, TFM, or CE is through P_{TWM}.

CONCLUSIONS

Based on the functional crosslinking monomer NOBE, a TBM-imprinted nanowire membrane was first prepared in an AAO membrane by template synthesis. However, the control nanowire membrane exhibited a different morphology and took on a particulate appearance. Overall, this method eliminated the need for additional functional monomers and empirical optimization of relative ratios of functional monomers, crosslinkers, and templates. The TBM-imprinted nanowire membrane exhibited high transport selectivity for TBM compared to the control granular membrane. This characteristic would also be applicable to assays of TBM residue by using the nanowire membrane as a recognition element in sensors.

References

1. Penmetsa, K. V.; Leidy, R. S.; Shea, D. J Chromatogr A 1997, 766, 225.
2. Corcia, A. D.; Crescenzi, C.; Samperi, R.; Scappaticcio, L. Anal Chem 1997, 69, 2819.
3. Wulff, G. Angew Chem Int Ed Engl 1995, 34, 1812.
4. Kempe, M.; Mosbach, K. Tetrahedron Lett 1995, 36, 3563.
5. Haupt, K. Chem Commun 2003, 21, 171.
6. Alvarez-Lorenzo, C.; Concheiro, A. J Chromatogr B 2004, 804, 231.
7. Bastide, J.; Cambona, J. P.; Breton, F.; Piletsky, S. A.; Rouillon, R. Anal Chim Acta 2005, 542, 97.
8. Matsui, J.; Akamatsu, K.; Hara, N.; Miyoshi, D.; Nawafune, H.; Tamaki, K.; Sugimoto, N. Anal Chem 2005, 77, 4282.
9. Shi, H. Q.; Tsai, W. B.; Garrison, M. D.; Ferrari, S.; Ratner, B. D. Nature 1999, 398, 593.
10. Ulbricht, M. J Chromatogr B 2004, 804, 113.
11. Huang, J. Y.; Wei, Z. X.; Chen, J. C. Sens Actuators B 2008, 134, 573.
12. Hillberg, A. L.; Brain, K. R.; Allender, C. J. J Mol Recognit 2009, 22, 223.
13. Yilmaz, E.; Haupt, K.; Mosbach, K. Angew Chem Int Ed Engl 2000, 39, 2115.
14. Titirici, M. M.; Hall, A. J.; Sellergren, B. Chem Mater 2002, 14, 21.
15. Titirici, M. M.; Hall, A. J.; Sellergren, B. Chem Mater 2003, 15, 822.
16. Yang, H. H.; Zhang, S. Q.; Tan, F.; Zhuang, Z. X.; Wang, X. R. J Am Chem Soc 2005, 127, 1378.
17. Li, Y.; Yang, H. H.; You, Q. H.; Zhuang, Z. X.; Wang, X. R. Anal Chem 2006, 78, 317.
18. Sibrian-Vazquez, M.; Spivak, D. A. J Am Chem Soc 2004, 126, 7827.
19. Wang, H. J.; Zhou, W. H.; Yin, X. F.; Zhuang, Z. X.; Yang, H. H.; Wang, X. R. J Am Chem Soc 2006, 128, 15954.
20. Sibrian-Vazquez, M.; Spivak, D. A. Macromolecules 2003, 36, 5105.
21. Krotz, J. M.; Shea, K. J Am Chem Soc 1996, 118, 8154.
22. Chen, C. B.; Chen, Y. J.; Zhou, J.; Wu, C. H. Anal Chim Acta 2006, 569, 58.